RECENT EXPLORATIONS IN RELAXATION METHODS FOR THREEDIMENSIONAL TRANSONIC POTENTIAL FLOW *

W. SCHMIDT**, S. HEDMAN***

SUMMARY

In the past relaxation methods have been demonstrated to be a powerful numerical tool for obtaining steady-state solutions to the transonic potential equation. Till now the main efforts were in the development of quite general analysis procedures while this paper presents a method for the analysis as well as the design problem in threedimensional transonic flow. On arbitrary sub-portions of the configuration shape or pressure might be prescribed. This allows the method to be applied in aerodynamic design studies with the physical relevant quantities being changed.

By use of this procedure a wing body combination has been designed and tested in the windtunnel. Comparing the experimental results with the theoretically predicted ones different effects are shown and the proof of assumptions is discussed.

ÜBERSICHT

Relaxationsverfahren haben sich in den letzten Jahren als sehr wirksame Methoden zur numerischen Lösung der stationären transsonischen Potentialgleichungen erwiesen. Bisher galt das Interesse der Entwicklung von allgemein verwendbaren Nachrechnungsverfahren während dieser Vortrag ein Verfahren vorstellen wird, mit dem sowohl die Nachrechnungs- als auch die Entwurfsaufgabe in dreidimensionaler transsonischer Strömung gelöst werden kann. Dabei können auf beliebigen Teilgebieten des Flügels Druck oder Kontur vorgegeben werden, was die Verwendung bei aerodynamischen Entwurfsstudien besonders attraktiv macht.

Mit Hilfe dieses Verfahrens wurde eine Flügel-Rumpf Kombination entworfen und nach Herstellung eines Modelles im Windkanal getestet. Der Vergleich der gemessenen Druckverteilungen mit den vorher berechneten enthält die kritische Diskussion verschiedener Effekte und den Nachweis getroffener Vereinfachungen.

RESUME

Les années passées il a été montré que les méthodes de relaxation sont un outil numérique puissant pour obtenir des solutions stationaires de l'équation potentielle transonique. Jusqu'à présent les plus grands efforts ont été dérigés vers le développement de procédés d'analyse assez généraux tandis que cette communication présente une méthode valable aussi bien pour le problème d'analyse que celui de dessin en écoulement tridimensionel transonique. Sur des parties arbitraires de la configuration on peut imposer la forme géométrique ou la pression. Ceci permet d'appliquer la méthode à des études de dessin aérodynamique en changeant les quantités physiques importantes.

En utilisant ce procédé une combination aile-fuselage a été dessinée et contrôlée en soufflerie En comparant les résultats expérimentaux avec les prédictions théoriques différents aspects sont mis en évidence et la preuve des hypothèses est discutée.

1. INTRODUCTION

In the past few years numerical techniques for the computation of the inviscid transonic potential flow attained a high state of development. Mathematically, the description of steady transonic flows requires the solution of "mixed" equations, which are elliptic in subsonic regions and hyperbolic in supersonic ones. The problem is essentially nonlinear and solutions generally contain discontinuities representing shock waves. The basic numerical procedure used is that first introduced by Murman and Cole [1]. It accounts for the mixed elliptic-hyperbolic character of the governing equations by using a mixed finite difference scheme. The general procedure is to employ centered differences when the flow is locally subsonic and one-side differences when it is locally supersonic.

Using line relaxation different methods have been developed to solve as well the full potential equation as the small perturbation form. Threedimensional results have been given for lifting wings and also for lifting wing-body combinations [2-8]. First attempts have been made also to take in account windtunnel wall effects [3, 9] and threedimensional viscous effects [9, 10].

* The research reported herein was sponsored jointly by the Air Material Department of the Swedish Defence Material Administration and the German Ministry of Defense (ZTL contract T/R 720/R 7600/42009)

** Dornier GmbH, D-7990 Friedrichshafen, Postfach 1420

*** The Aeronautical Research Institute of Sweden, FFA, S-16111 Bromma 11, P.O. Box 11021

The present paper will show the development of a threedimensional transonic design relaxation method basing on the previous work. In wing design, generally, planform, Mach number and lift coefficient are prescribed for the design point. From two-dimensional design studies a desireable chordwise goal pressure distribution is conceived.

Either analysis methods can be applied iteratively to finally give the wing shape or design methods have to be used the threedimensional pressure distribution being fed in and the wing section shapes being calculated. The first approach is being pursued at NASA AMES [11] using an optimizer in combination with the AMES analysis method. For given constraints pressure distribution and shape are computed which produce minimum drag. Our approach will follow along the second line. The procedure and program development has been described in [12] in detail.

2. TRANSONIC POTENTIAL THEORY

We begin the discussion of our threedimensional transonic relaxation method by considering the different assumptions behind the steady transonic perturbation equation and the boundary conditions. The validity of those assumptions is proved by error estimates for the type of flow being of interest.

2.1 Basic Equations

The threedimensional steady velocity potential Φ is expanded as

$$\Phi(x,y,z) = U_\infty \{x+\varepsilon\phi\ (x,y,z)\} \qquad (1)$$

using a scaling factor $\varepsilon = \delta^{2/3}/M_\infty$, δ being some mean relative thickness value.

Looking in detail at the velocity distributions being considered for supercritical wing flow as shown in figure 1 we can state that

- o square terms of disturbance velocities are small compared with one, $\varepsilon^2\phi_x^2$, $\varepsilon^2\phi_y^2$ $\varepsilon^2\phi_z^2 << 1$
- o disturbance velocities are not small compared with one, but $(\kappa-1)\ M_\infty^2\ \varepsilon\phi_x << 1$
- o $\frac{\kappa-1}{2} M_\infty^2\varepsilon^2\ (\phi_y^2+\phi_z^2) << (1-M_\infty^2)$, except if M_∞ is close to one
- o $\frac{\kappa+1}{2} M_\infty^2\varepsilon^2\phi_x^2$ is not $<< (1-M_\infty^2)$

This finally leads to the perturbation equation in the disturbance potential.

$$\{(1-M_\infty^2)-(\kappa+1)M_\infty^2\varepsilon(1+\tfrac{\varepsilon}{2}\phi_x)\ \phi_x\}\ \phi_{xx} + \phi_{yy} + \phi_{zz} - 2M_\infty^2\varepsilon\ \{\phi_y\phi_{xy}+\phi_z\phi_{xz}\} = 0 \qquad (2)$$

If in addition the assumptions

- o $\varepsilon\phi_x$, $\varepsilon\phi_y$, $\varepsilon\phi_z << 1$
- o $\varepsilon\phi_y\phi_{xy}$, $\varepsilon\phi_z\phi_{xz} << \{\ \}\ \phi_{xx}$

would be valid, equation (2) would simplify to the well known classical small disturbance equation

$$\{(1-M_\infty^2)-(\kappa+1)M_\infty^2\varepsilon\phi_x\}\ \phi_{xx} + \phi_{yy} + \phi_{zz} = 0 \qquad (3)$$

Knowing that equation (2) is not consistent in the sense of second or higher order expansions it should be kept in mind that it is a better approximation to the full potential equation as far as the residual error terms are concerned for the classes of wings mentioned.

2.2 Boundary Conditions

Flow tangency condition at the surface with its local normal vector $\vec{n}$ including the angle of attack is expressed as

$$(1+\varepsilon\phi_x)n_x + \varepsilon\phi_y n_y + \varepsilon\phi_z n_z = 0 \qquad (4)$$

From the previous chapter it is known that $\varepsilon\phi_x$, $\varepsilon\phi_y$, $\varepsilon\phi_z$ are not small compared with one any more, i.e. simplifications of equation (4) are only allowed if $n_y << n_z$. Figure 2 shows that this is not true for swept wings due to the sweep angle or due to the variation of thickness in spanwise direction.

Therefore we do not intend to use the classical linearized wing boundary condition for highly loaded swept wings.

For arbitrarily shaped closed bodies it is well known that none of the terms in equation (4) can either be simplified or neglected. Only for infinite long bodies with no change in cross section with length equation (4) can be simplified to

$$\phi_y n_y + \phi_z n_z = 0 \qquad (5)$$

The wake boundary condition is included in the well known way neglecting wake curvature as shown in previous publications [6].

2.3 Far Field Solutions

Not using any transformations to put infinity to a finite domain we have to introduce far field solutions along the boundaries of the domain in which the flow field has to be calculated from the potential equation. Those far field solutions have to satisfy the flow field between the finite domain and infinity. Some distance away from the configuration the subsonic flow field can be described by the linear potential equation. Therefore classical source and vortex methods can be used.

The most classical way is that of Klunker, unfortunately mismatching the normal velocities ϕ_z resp. ϕ_y along the farfield boundaries. Instead, a wing vortex lattice giving ϕ_y, ϕ_z can be used [9] or a full solution along the boundary applied [13].

To simulate the presence of wind tunnel walls wall conditions can be included as described in [9].

2.4 Pressure Coefficients

Consistent with the assumptions which led to the basic perturbation equation (2) the isentropic pressure coefficient relationship is reduced by second order series expansion to

$$c_p = - \{2\varepsilon\phi_x+(1-M_\infty^2)\varepsilon^2\phi_x^2+\varepsilon^2(\phi_y^2+\phi_z^2)\} \qquad (6)$$

Forces and moments can be integrated by numerical means from the local pressures.

3. DESIGN PROCEDURE

Designing a new wing, generally planform, design point lift coefficient and Mach number are given. From twodimensional studies also a desired design-pressure distribution for the threedimensional wing is given. The core of the design process is now to find the wing section shapes that produce such pressure distributions. While this can be done by trial and error using an analysis procedure as described in the previous chapter, it is more efficient to have a design method available, in which the pressure distribution is the given boundary condition, while the shape i.e. the normal velocity component is the unknown.

This classical Dirichlet problem is generally solved by prescribing the tangential velocity $u=\phi_x$ instead of the normal velocity component as boundary condition. From own twodimensional studies it was found that in a relaxation procedure this way seems to fail, the reason being the a priori unknown potential distribution in front of the wing. Instead in a similar manner like Steger und Klineberg [14] and Langley [15] for aerofoil design also for wing design the vorticity equation can be used as an intermediate step which must be fulfilled. The steps in such a design procedure are

- o prescribe pressure c_p
- o from similar solutions or iteratively suggest the velocities ϕ_y and ϕ_z
- o calculate the tangential velocity ϕ_x from the given c_p eq. (6) by use of ϕ_y, ϕ_z from the second step
- o for use in the vorticity equation

  $$\phi_{xz} = \phi_{zx}$$

  calculate the cross derivative ϕ_{xz} by differentiation in z
- o now integrate in x-direction to get a boundary condition in ϕ_z

  $$\phi_z = \int \phi_{xz}\, dx$$

  to have a Neumann type direct boundary condition.

By such a procedure the inverse problem is reduced to a direct one which can be solved by the standard procedure.

4. NUMERICAL PROCEDURE

The basic feature of the numerical method is to solve the transonic perturbation equation in a rectangular grid box with variable mesh size as shown in fig. 3. Like in the twodimensional method of Murman and Cole [1] we account for the mixed elliptic-hyperbolic nature of the equation by central differences for the streamwise derivatives when the equation is elliptic and backward when the equation is locally hyperbolic. The y- as well as the z-derivatives are replaced everywhere by second order central differences.

The resulting set of nonlinear algebraic equations is solved iteratively be line relaxation. Each line forms an equation with a tridiagonal matrix for which fast solution procedures exist. For hyperbolic points under-relaxation ($\omega = 0.7 \div 0.9$) is used, for elliptic points over-relaxation ($\omega = 1.7 \div 1.9$)

$$\phi^{\nu+1} = \phi^{\nu} + \delta \{\phi^{\nu+\frac{1}{2}} - \phi^{\nu}\}$$

The scheme is fully conservative and for shock points a shock point operator is used.

5. MODEL DESIGN AND TESTING

To have detailed experimental data to compare the described method with and to show its applicability to threedimensional wing design a wind tunnel model within the PT-series [16] was designed and tested. A three side view of this PT7-model is shown in figure 4. It consists of a cylindrical body with a low mounted trapezoidal swept wing (AR = 4, $\lambda = 0.4$, $\phi_{25} = 35^0$). The design goal was to reach at $M_\infty = 0.9$ a lift coefficient of 0.2 having a relative thickness of > 9 % in streamwise direction. The pressure distribution was assumed to be of roop-top type with parallel isobars and a local Mach number ahead of the shock M < 1.30.

The numerical design proceeded along the following lines:

- o A basic guess for the wing section shape is taken from a twodimensional airfoil having the prescribed properties.

This led to a threedimensional pressure distribution with a too strong inboard shock and a too small front loading in the tip section.

- o Prescribe upper surface pressure distribution retaining lower surface shape. The results are reasonable pressure distributions but section shapes which do not close (too thick or negative thickness).
- o Rotate lower surface around section nose points to obtain closure.

This led to a reasonable pressure distribution except at the most outboard stations but with a too small plateau and a thin last 20 % of chord for the root section due to the concave upper surface (see figure 5).

- Add thickness to the lower surface in the root region, modify nose shape, change twist to get thicker trailing edge portions, extended plateaus, improved tip section.

The result turned out to be almost the final design. Now a geometry definition package [17] was used to get smooth, continuous surfaces. Repeated applications of the analysis program and definition package had to insure that the geometry changes did not destroy the target pressure distribution. The final shape and pressure distribution can be seen from figure 6. The final thickness distribution is shown in figure 7.

Verifying this geometry a windtunnel model was built at FFA and tested extensively in the FFA S4 transonic wind tunnel (figure 8). Balance tests and pressure measurements have been carried out at Reynolds numbers of $1.1\text{-}1.8 \cdot 10^6$ within a Mach number range of 0.5-0.97. Pressure measurements were done at three chordwise sections 1,2,3 being at the same span stations as the computational sections 5,10,16. Oil flow pictures were taken to show the presence of shocks and shock induced separation. To get at least some information about the behaviour at higher Reynolds numbers three different transition positions were tested. At first transition was fixed 8 mm behind the leading edge by use of 0.2 mm spheres mounted with 4 mm spacing, secondly tests were performed with free transition and a third set of tests was done with fixed transition at 50 % chord using a band of carborundum grains with 0.2 mm diameter.

6. RESULTS

A detailed description of the test results and the comparison with computed pressures and forces as well as the boundary layer behaviour will be given in reference 18. The present paper will give only a first comparison between previously computed design pressure distributions and the experimentally verified ones. While preparing this paper not all of the mentioned experimental results were available.

Figure 9 shows the oil flow pattern for the design point $M_\infty = 0.9$, $\alpha = -1^o$ and fixed transition at 8 mm behind the leading edge. A shock is present almost parallel to the trailing edge with a strong cross flow behind the shock in the inner 50 % of the halfspan but with no separation. On figure 10 the pattern for $\alpha = 0^o$ indicate a much stronger shock almost at the same location but with separation behind the shock. As indicated in more detail on figure 11 which shows only the innermost part of the pattern at $\alpha = 0^o$ the shock and separation starts approximately at 20 % halfspan of the exposed wing.

The measured pressures for $\alpha = -1^o$ and $M_\infty = 0.899$ are shown on figures 12 a-c. For comparison the previously calculated design-pressures are included as solid lines. The computed lift and drag coefficients for the inviscid flow with shock point operator were $C_L = 0.27$ and $C_D = 0.01$ while the experimental ones were measured as $C_L = 0.23$ and $C_D = 0.023$. Measured and calculated pressures agree quite well especially keeping in mind that in the quite coarse mesh with 41 x 28 x 29 points in x-y-z direction section 1 containes only 14 points along its chord, section 3 even only 11 points, starting at 5 % local chord. This will explain the differences at the leading edge. Shock position and trailing edge pressures are influenced by viscous effects which are not included in the theoretical results yet. A more detailed analysis using threedimensional boundary layer method and the displacement thickness concept as shown in ref. 9 will give better agreement at least for the shock position in station 1. The tendency of a theoretically predicted shock position with less sweep along span can be explained by the lack of the cross terms in eq. (2). It should be kept in mind that all the theoretical results shown in the present paper were computed using eq. (3), due to some problems in finding the proper operators for eq. (2) which did not give results while this paper was prepared.

Figures 13 a-c include the comparisons for $M_\infty = 0.9$ and $\alpha = 0^o$. The agreement still is quite good and the different deviations can be explained in the same way. The shocks are stronger but nearly remain at the same chordwise position. While for $M_\infty = 0.9$ and $\alpha = -1^o$ the maximum local Mach numbers were calculated to be less or equal 1.3, for $\alpha = 0$ the local Mach numbers ahead of the shock were larger than 1.3. First threedimensional boundary layer calculations also indicated no separation for $\alpha = -1^o$ using the theoretical pressure distribution while there seemed to be separation for $\alpha = 0^o$ starting at 20 % halfspan of the exposed wing. Finally figures 14 and 15 show the comparisons for the lower Mach number $M_\infty = 0.87$ and $\alpha = 0^o$, resp. $\alpha = 1^o$. Again, the measured pressures agree quite well with those theoretically predicted before the experimental data were known.

7. CONCLUSION

A transonic analysis and design method was developed and tested by designing the transonic wing body configuration PT7. Detailed wind tunnel experiments verified the design pressures and proved the computational method to be a helpful tool in transonic aerodynamic aircraft design. Still some improvements on the method have to be done to give better results for highly loaded swept and tapered wings.

This goal can be reached by developing a method which solves the full potential equation but it seems to be sufficient to include some more terms in the perturbation equation as indicated by eq. (2). Pay-off would be a much faster numerical method than solving the full potential equation.

Basing on the present PT7 design a more elaborate redesign will be done in the near future including boundary layer calculations and the improved potential flow method. Also, the design pressure distribution will be changed to a more realistic one having better rear loading and an improved nose shape.

8. REFERENCES

[1] Murman, E.M.; Cole, J.D.
Calculation of Plane Steady Transonic Flows
AIAA Journal, Vol . 9, No. 1, 1971, pp 114-121

[2] Bailey, F.R.; Ballhaus, W.F.
Comparisons of Computed and Experimental Pressures for Transonic Flows about Isolated Wings and Wing-Fuselage Configurations
NASA SP-347, 1975, pp 1213-1232

[3] Newman, P.A.; Klunker, E.B.
Numerical Modeling of Tunnel-Wall and Body-Shape Effects on Transonic Flows over Finite Lifting Wings
NASA SP-347, 1975, pp 1189-1212

[4] Albone, C.M.; Hall M.C.; Gaynor Joyce
Numerical Solution for Transonic Flows Past Wing-Body Combinations
Symposium Transsonicum II, Göttigen 1975, Springer Verlag

[5] van de Vooren, J.; Slooff, H.W.; Huizing, G.H.; van Essen, A.
Remarks on the Suitability of Various Transonic Small Perturbation Equations to Describe Three-dimensional Transonic Flow
Symposium Transsonicum II, Göttingen 1975, Springer Verlag

[6] Schmidt, W.; Vanino R.
The Analysis of Arbitrary Wingbody Combination in Transonic Flow Using a Relaxation Method
Symposium Transsonicum II, Göttingen 1975, Springer Verlag

[7] Jameson, A.
Numerical Computation of Transonic Flows with Shock Waves
Symposium Transsonicum II, Göttingen 1975, Springer Verlag

[8] Sedin, Y.; Karlsson, K.
Some Numerical Resuslts of a New Threedimensional Transonic Flow Method
Symposium Transsonicum II, Göttingen 1975, Springer Verlag

[9] Schmidt, W.; Stock, H.-W.; Fritz W.
Numerical Simulation of Threedimensional Transonic Flow Including Wind Tunnel Wall Effects
AGARD Specialists Meeting "Numerical Methods and Wind Tunnel Testing", VKI Brussels, 1976

[10] Hedman, S.
Pressure Distributions for a Swept Wing Body Configuration Obtained from Coupling Transonic Potential Flow Calculations and Boundary Layer Calculations
to be published at AGARD Symposium "Prediction of Aerodynamic Loading", NASA AMES Moffett Field, Sept. 1976

[11] Murman, E.M.; Hicks, R.M.; Vanderplaats, G.N.
Application of Numerical Optimization to Airfoil Design
NASA SP-347, pp 749-768, 1975

[12] Hedman, S.; Stock, H.-W.; Fritz, W.; Schmidt, W.
Entwurfsverfahren für dreidimensionale reibungsbehaftete transsonische Strömungen
Dornier FB 75/45 B, 1975, FFA AU-1043

[13] Dickson, L.J.; Chen, A.W.; Rubbert, P.E.
A New Approach to Far Field Boundary Conditions in Transonic Computations
5th International Conference on Numerical Methods in Fluid Dynamics, Enschede, 1976

[14] Steger, J.L.; Klineberg, J.M.
A Finite-Difference Method for Transonic Airfoil Design
AIAA Paper 72-679, 1972

[15] Langley, M.J.
Numerical Methods for Twodimensional and Axisymmetric Transonic Flows
ARA Memo 143, 1973

[16] Gustavsson, A.L.; Hedman, S.
Design and Test of Sonic Roof-Top Pressure Distribution Wing
Symposium Transsonicum II, Göttingen 1975, pp 273-280, Springer Verlag

[17] Maisel, M.; Nagel, J.
Numerische Definition von dreidimensionalen Flächen
Dornier Note, 1976

[18] Hedman, S.; Schmidt, W.
Results and Analysis of the Design and Testing of the PT7 Transonic Wing-Body Combination
to be published as FFA and Dornier Report, 1976

9. FIGURES

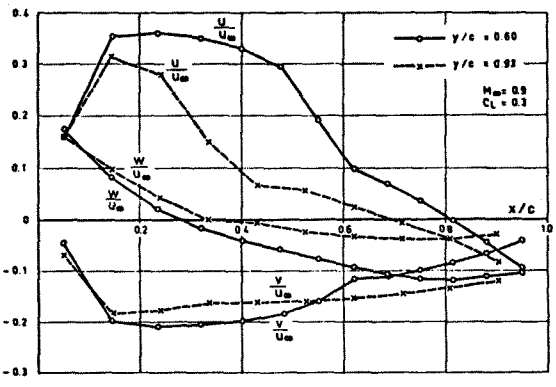

Figure 1: Velocity distribution for two sections

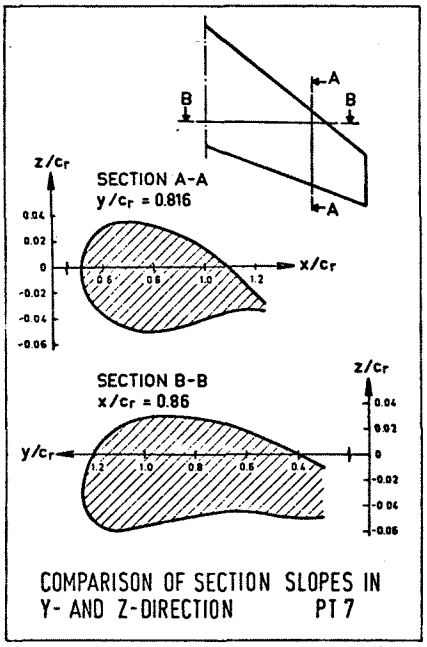

Figure 2: Ratio of normal vector components n_x, n_y, n_z

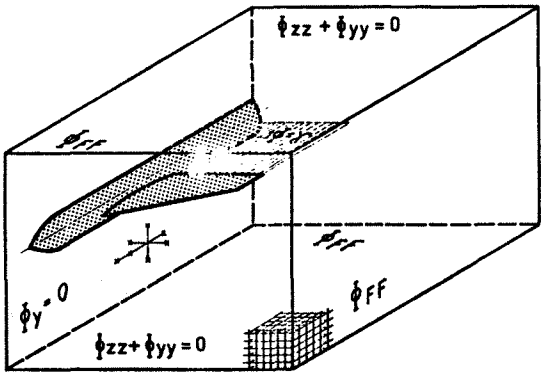

Figure 3: Computational grid system for the present TSP method

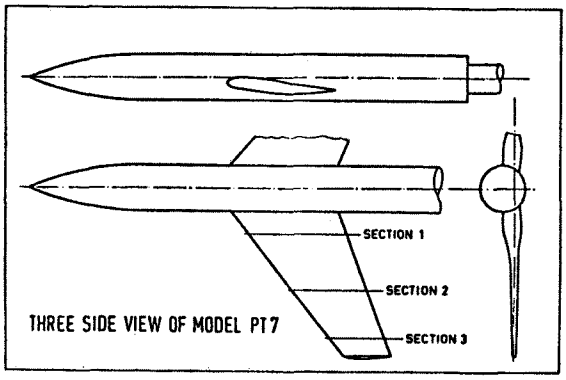

Figure 4: Schematic drawing of PT7 with sections for pressure taps

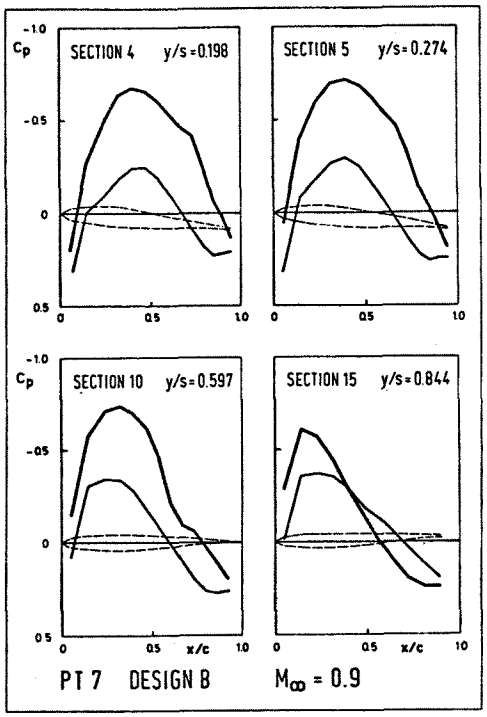

Figure 5: Intermediate design pressures and section shapes

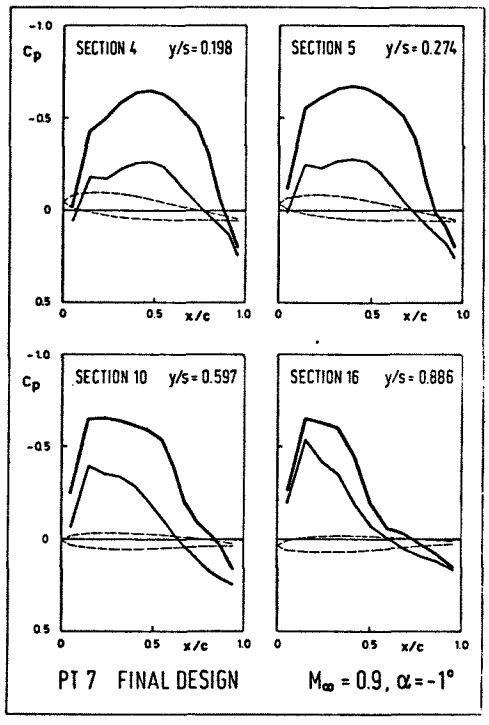

Figure 6: Final design features

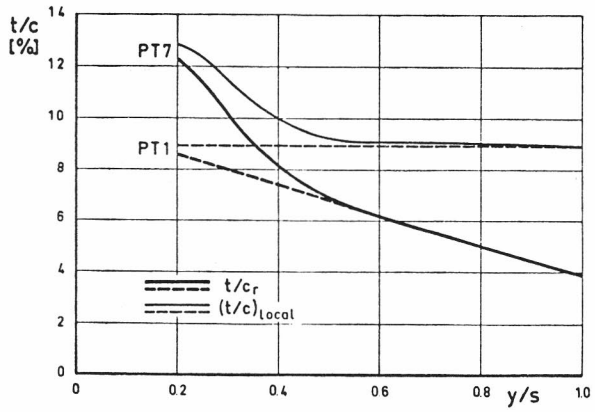

Figure 7: Maximum thickness distribution for PT1 and PT7

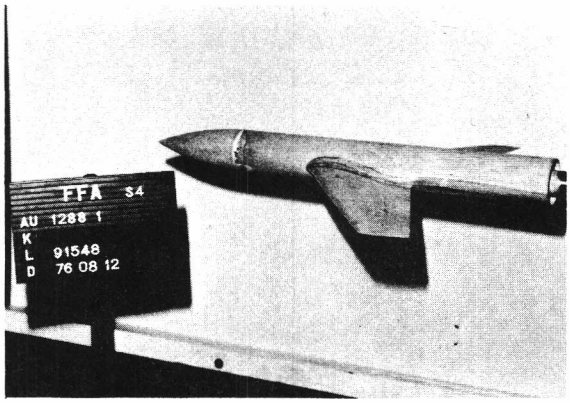

Figure 8: Windtunnel model PT7 in FFA S4 tunnel

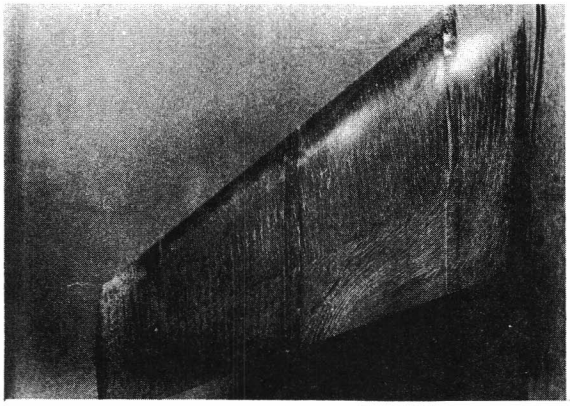

Figure 9: Oil flow pattern for $M_\infty = 0.9$, $\alpha = -1^o$

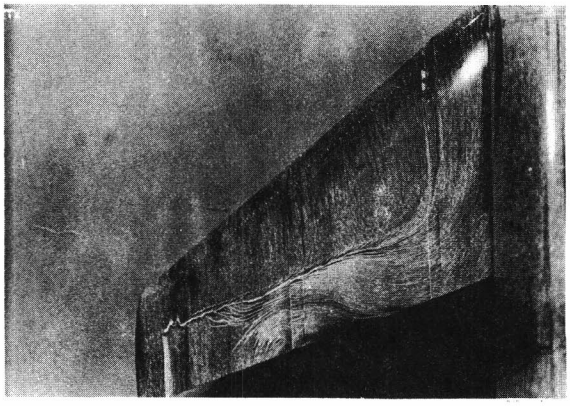

Figure 10: Oil flow pattern for $M_\infty = 0.9$, $\alpha = 0^o$

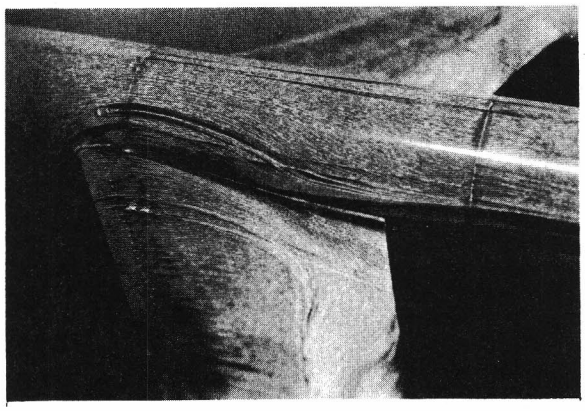

Figure 11: Oil flow pattern in the wing root region $M_\infty = 0.9$, $\alpha = 0^o$

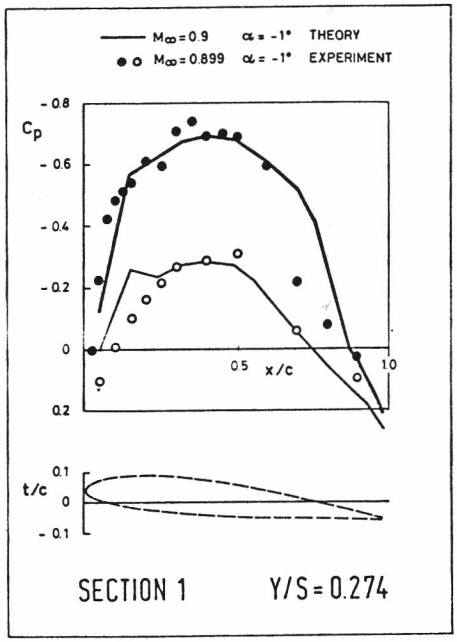

Figure 12 a-c: Comparison of pressure distribution at $M_\infty = 0.9$, $\alpha = -1^o$

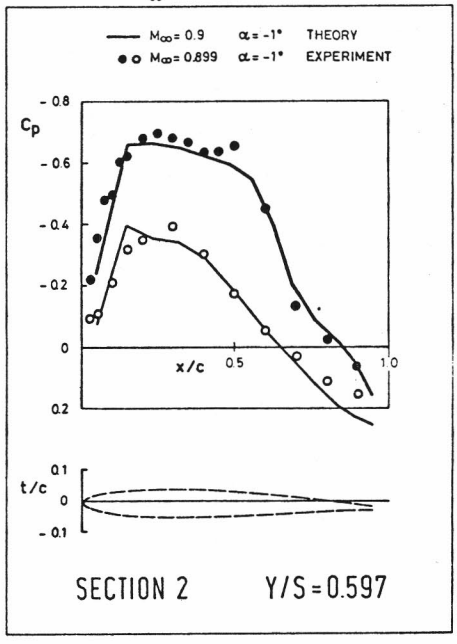

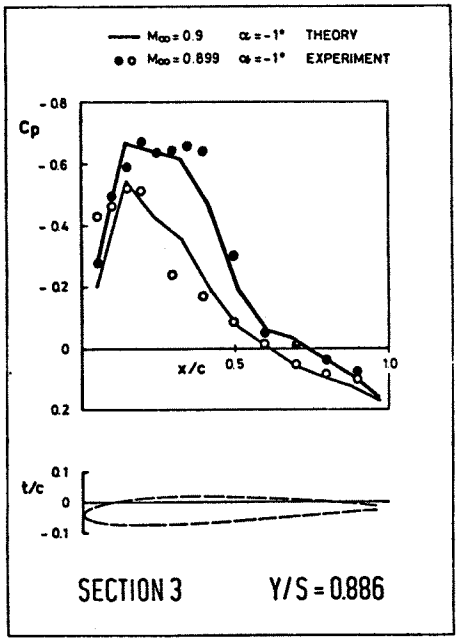

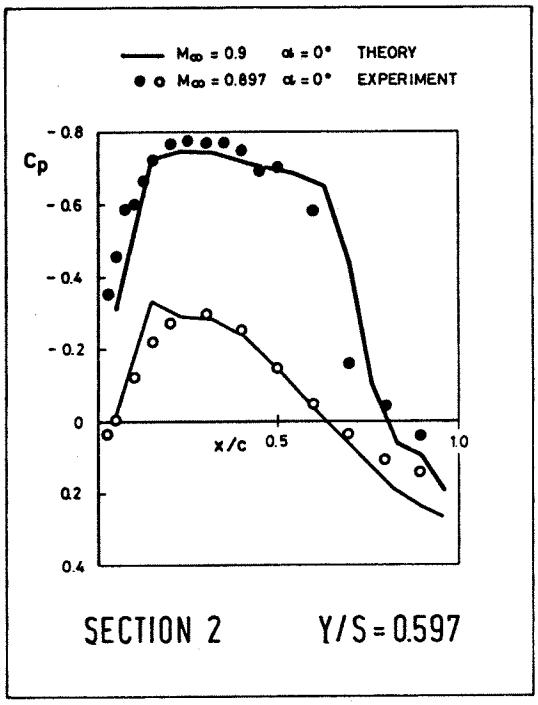

Figure 13 a-c: Comparison of pressure distribution at $M_\infty = 0.9$, $\alpha = 0^0$

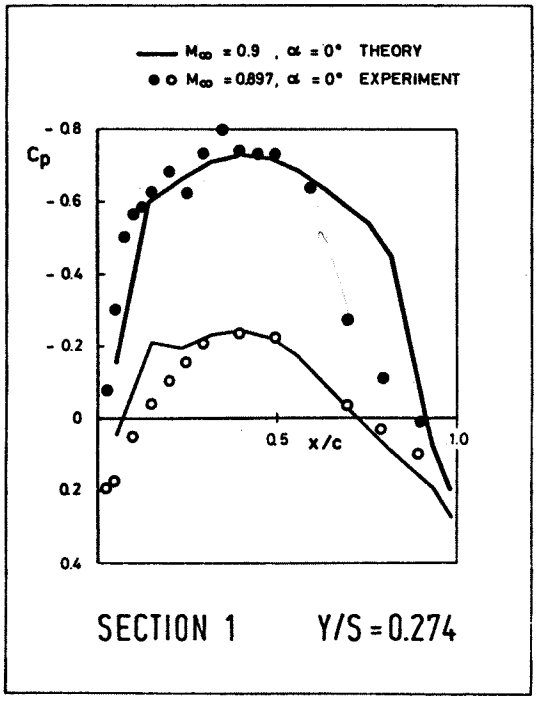

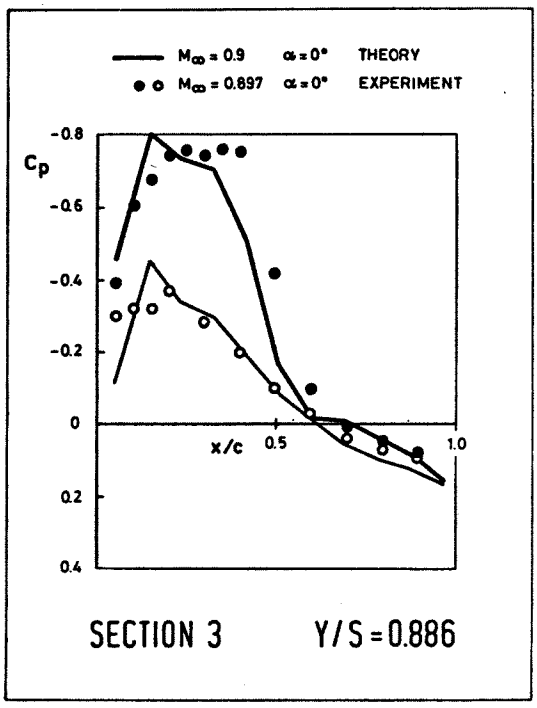

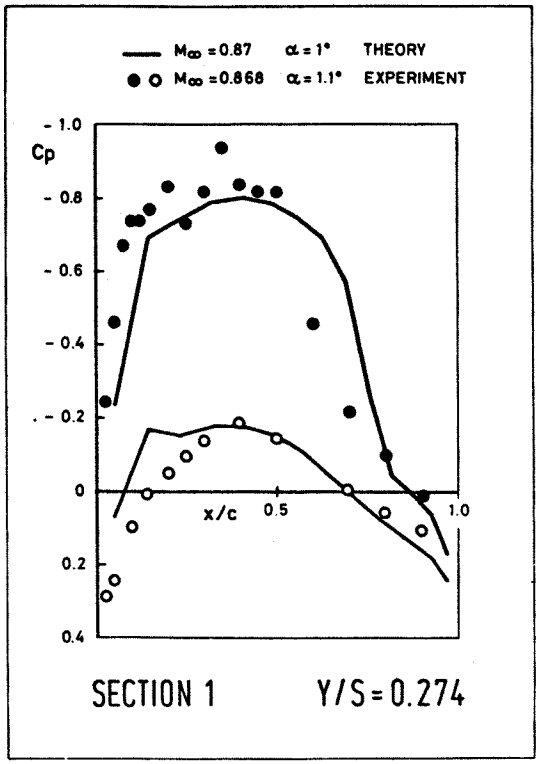

Figure 14: Comparison of pressures at section at $M_\infty = 0.87$, $\alpha = 0^o$

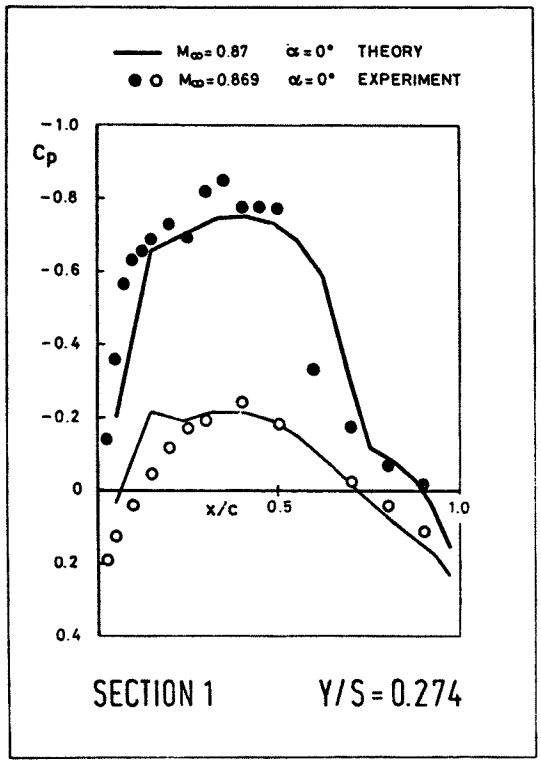

Figure 15: Comparison of pressures at section at $M_\infty = 0.87$, $\alpha = 1^o$